A Novel Near-Real-Time Quality-Control Procedure for Radiometric Profiles Measured by Bio-Argo Floats: Protocols and Performances

EMANUELE ORGANELLI,* HERVÉ CLAUSTRE,* ANNICK BRICAUD,* CATHERINE SCHMECHTIG,+ ANTOINE POTEAU,* XIAOGANG XING,#,@ LOUIS PRIEUR,* FABRIZIO D'ORTENZIO,* GIORGIO DALL'OLMO,&,** AND VINCENZO VELLUCCI*

* *Sorbonne Universités, UPMC Université Paris 06, CNRS, UMR 7093, Laboratoire d'Océanographie de Villefranche, Villefranche-sur-Mer, France*
+ *Sorbonne Universités, UPMC Université Paris 06, CNRS, UMS 3455, OSU Ecce-Terra, Paris, France*
# *Key Laboratory of Physical Oceanography, Ocean University of China, Qingdao, China*
@ *Takuvik Joint International Laboratory, CNRS, Université Laval, UMI 3376, Québec City, Québec, Canada*
& *Plymouth Marine Laboratory, Plymouth, United Kingdom*
** *National Centre for Earth Observation, Plymouth Marine Laboratory, Plymouth, United Kingdom*

(Manuscript received 25 September 2015, in final form 17 February 2016)

ABSTRACT

An array of Bio-Argo floats equipped with radiometric sensors has been recently deployed in various open ocean areas representative of the diversity of trophic and bio-optical conditions prevailing in the so-called case 1 waters. Around solar noon and almost every day, each float acquires 0–250-m vertical profiles of photosynthetically available radiation and downward irradiance at three wavelengths (380, 412, and 490 nm). Up until now, more than 6500 profiles for each radiometric channel have been acquired. As these radiometric data are collected out of an operator's control and regardless of meteorological conditions, specific and automatic data processing protocols have to be developed. This paper presents a data quality-control procedure aimed at verifying profile shapes and providing near-real-time data distribution. This procedure is specifically developed to 1) identify main issues of measurements (i.e., dark signal, atmospheric clouds, spikes, and wave-focusing occurrences) and 2) validate the final data with a hierarchy of tests to ensure a scientific utilization. The procedure, adapted to each of the four radiometric channels, is designed to flag each profile in a way compliant with the data management procedure used by the Argo program. Main perturbations in the light field are identified by the new protocols with good performances over the whole dataset. This highlights its potential applicability at the global scale. Finally, the comparison with modeled surface irradiances allows for assessing the accuracy of quality-controlled measured irradiance values and identifying any possible evolution over the float lifetime due to biofouling and instrumental drift.

1. Introduction

The Argo program is an international network launched in 1999 with the aim of increasing the observations of key physical properties (i.e., temperature T and salinity S) across the global ocean through the use of autonomous profiling platforms. Today, more than 3500 Argo floats are routinely delivering (every 10 days) T and S profiles for the upper 2000 m of the water column in very diverse open ocean systems (Freeland et al. 2010). After the launching of the Argo program, some exploratory studies began to use profiling floats as platforms to also document biogeochemical and biological properties through the acquisition of time series in key locations (Körtzinger et al. 2004; Boss et al. 2008; Bishop and Wood 2009). The so-called Bio-Argo floats, based on Argo floats but equipped with optical and bio-optical sensors, today represent a mature technology for monitoring some biological and bio-optical variables from the surface to the ocean interior at unprecedented temporal and spatial resolutions (Johnson et al. 2009; Claustre et al. 2010b; Claustre 2011).

Part of the existing Bio-Argo array is able to acquire photosynthetically available radiation (PAR) and downward

Corresponding author address: Emanuele Organelli, Laboratoire d'Océanographie de Villefranche, 181 Chemin du Lazaret, 06230 Villefranche-sur-Mer, France.
E-mail: emanuele.organelli@obs-vlfr.fr

DOI: 10.1175/JTECH-D-15-0193.1

irradiance (E_d) measurements at three wavelengths in the UV and blue spectral ranges, in addition to other variables such as chlorophyll-*a* and dissolved oxygen concentrations. The rationale to have radiometric observations on profiling floats is twofold. First, irradiance and other radiometric quantities are key environmental parameters for addressing the variability of biological processes and for defining the bio-optical status of open ocean upper water masses. Second, radiometric measurements are also a source of data for validating ocean color radiometry measurements and biogeochemical products from space (Claustre et al. 2010a).

For a global ocean observation system (Johnson et al. 2009), standardized data processing procedures and public availability of quality-controlled Bio-Argo data for the end-user community are essential (Johnson et al. 2009; Claustre et al. 2010b). Among the measurements already implemented on Bio-Argo floats, radiometry has specific constraints that require a dedicated processing of data and an adaptation of the existing techniques. On cruises, where radiometric measurements have been mostly acquired to date, profiles are generally associated with the simultaneous acquisition of an above-water incident irradiance reference (Mueller et al. 2003). Above-water observations provide the required reference to unambiguously assign features in the vertical profile due to variations in surface irradiance (e.g., clouds). Once these features are identified and corrected, accurate estimates of in-water optical properties can be obtained (Mueller et al. 2003). In the case of floats, an above-water reference is not available. Another peculiarity of Bio-Argo measurements is that the float is generally not recovered. The postdeployment dark readings, a classical procedure carried out at the end of sea operations and used to verify instrument response over the time and to possibly correct data (Mueller et al. 2003), is thus not applicable on Bio-Argo floats.

Mueller et al. (2003) represents the most comprehensive handbook of protocols for quality-controlling radiometric measurements acquired in the traditional way, that is, from ships and under an operator's control. Recommended actions in data processing include, for example, dark signal corrections, depth offset adjustments, identification of perturbations in the light field induced by waves in the surface layer ("wave focusing" effect; Zaneveld et al. 2001), and atmospheric clouds along the profile (Mueller et al. 2003). Whereas certain NASA recommendations with respect to data acquisition can be easily followed with Bio-Argo floats (e.g., vertical profile down to at least 200 m, with high instrument sampling rate) or can be considered as negligible (e.g., depth offset adjustments between the pressure sensor and the radiometer), protocols concerning the identification of, for example, clouds and wave focusing need to be revised. Following these considerations, specific procedures to ensure scientific quality-controlled radiometric data from profiling floats have to be developed.

This is the purpose of the present study, which specifically focuses on the development of a new quality-control procedure for radiometric profiles [PAR and $E_d(\lambda)$ measurements] acquired by Bio-Argo floats and dedicated to bio-optical applications (i.e., which require calm sea and uniform sky conditions during the measurement; Mueller et al. 2003). The proposed procedure targets only profile shapes and is designed for near-real-time data distribution (i.e., within 24 h from sampling). More particularly, this quality-control procedure accounts for the identification of (i) dark signal along the profile; (ii) sporadic atmospheric clouds, wave-focusing, and spike occurrences; and (iii) measurements acquired under very unstable sky conditions. This procedure, which is potentially applicable to all Bio-Argo radiometric instruments and to any wavelength, differs from previous developed data analysis protocols for Bio-Argo floats (Xing et al. 2011, 2012) because each measurement is processed separately from the other radiometric acquisitions and independently from the vertical distribution of the other bio-optical quantities (e.g., chlorophyll-*a*). This procedure provides the final users with profiles that are quality-controlled and in which potential bad data are flagged in a way compliant with the Argo data management procedure (Schmid et al. 2007; Wong et al. 2013). No correction protocols for bad data are proposed here. Examples of processed data are shown for various areas and environmental conditions. Quality-control performance for a large array of Bio-Argo floats, deployed in various open ocean areas covering a wide range of bio-optical status, is also discussed. Finally, incident irradiance values above the surface derived from quality-controlled measurements are compared to modeled values for clear-sky conditions (Gregg and Carder 1990) in order to verify and discuss the accuracy of measured irradiance values over the float lifetime.

2. Instruments and data

The "PROVOR CTS-4" profiling float (Fig. 1) is the new generation of bio-optical and biogeochemical floats, specifically designed in the context of the Remotely-Sensed Biogeochemical Cycles in the Ocean (remOcean) and Novel Argo Ocean Observing System (NAOS) projects and subsequently adopted by several international collaborators or research programs (see acknowledgments). The platform conception was developed by NKE Marine Electronics Inc. (France). Compared to the previous PROVOR CTS-3 generation (Xing et al. 2011, 2012),

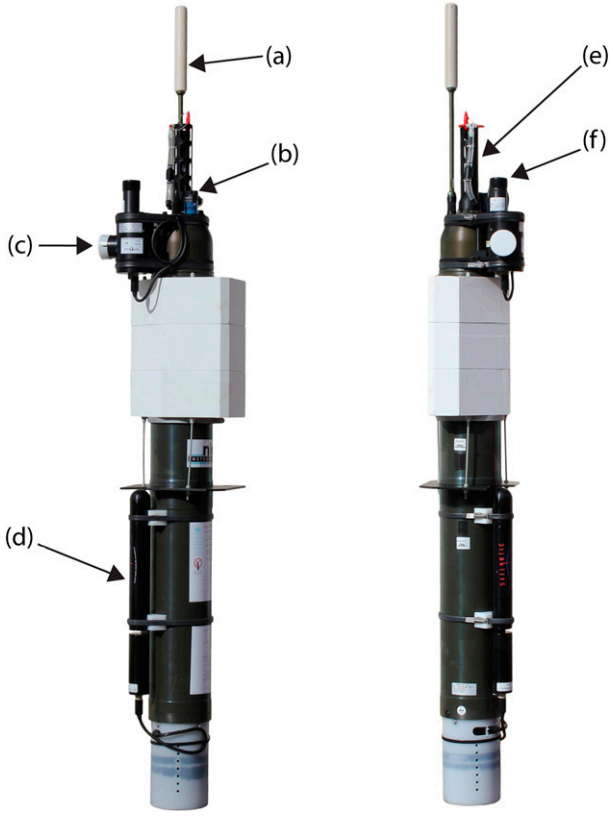

FIG. 1. The PROVOR CTS-4 free-drifting profiling float equipped with (a) Iridium antenna; (b) oxygen sensor; (c) sensor for chlorophyll fluorescence, chromophoric dissolved organic matter (CDOM) fluorescence, and particle light backscattering at 700 nm; (d) nitrate sensor; (e) conductivity–temperature–depth sensor; (f) radiometer [3 $E_d(\lambda)$ + PAR]. Photo by Thomas Jessin (Laboratoire d'Océanographie de Villefranche, France).

more variables are measured in this new configuration (i.e., PAR, nitrates, and dissolved oxygen) and, thanks to a new electronic device, the float displacement can be managed separately from the data acquisition. A detailed technical description can be found online (at http://www.obs-vlfr.fr/OAO/).

The new generation of PROVOR CTS-4 Bio-Argo floats is equipped with a multispectral ocean color radiometer (OCR-504, SATLANTIC Inc.) for measuring E_d at three wavelengths (i.e., 380, 412, and 490 nm) and PAR, integrated over 400–700 nm. Measurements are collected during upward casts programmed every 1, 2, 3, 5, or 10 days depending on the mission and scientific objectives. Generally, the cast starts from the parking depth at 1000 m at a time that is sufficient for surfacing around local noon. Specific missions are also programmed to acquire more than one profile per day (e.g., sunrise, noon, sunset). Radiometric measurements are acquired systematically in the upper 250 m of the cast. Data acquisition is nominally 1-m resolution between 10 and 250 m and increases at 0.20-m resolution between 10 m and the surface. Along with the factory calibration factors, electronic raw counts are transmitted to land through an Iridium two-way communication that also enables sampling strategy modifications. Radiometric quantities are then retrieved as follows (SATLANTIC 2013):

$$X = A_1(X_{\text{raw}} - A_0)\text{Im}, \tag{1}$$

where X represents the downward irradiance at 380, 412, or 490 nm (μW cm^{-2} nm^{-1}) or PAR (μmol quanta m^{-2} s^{-1}); X_{raw} are the raw counts for downward irradiance measurements or PAR; A_0 and A_1 are calibration coefficients; and Im is the immersion coefficient. Wavelength dependency is omitted for brevity. Factory calibration coefficients are specific to each radiometric channel of each sensor.

In this study, we used radiometric data collected between 8 November 2012 and 19 November 2014 by 65 Bio-Argo floats deployed in a variety of oceanic areas (Fig. 2) mainly corresponding to case 1 waters as defined by Morel and Prieur (1977). Finally, a total of 26 280 profiles (6570 profiles for each radiometric channel; Organelli et al. 2016) have been subjected to the quality-control procedure presented in the following sections and were used to discuss its performances. Raw data are publicly available online (at ftp://ftp.ifremer.fr/ifremer/argo/dac/coriolis/) and distributed as netCDF data files (Wong et al. 2013). The database is updated daily with new profiles.

3. Constraints of the Argo data management system to take into account

The quality-control procedure for radiometric profiles acquired by Bio-Argo floats, presented here, is developed also to cope with the general Argo data management procedure (Wong et al. 2013). Basically, a quality-controlled (QC) profile has to be generated from the raw field measurements by applying various tests for each data point (a given measurement at a given depth) acquired along the vertical profile and subsequently flagging them. Flags 1–4 have to be assigned: "1" for "good" records, "2" for "probably good" records, "3" for "probably bad" records, and "4" for "bad" records. Flag 3 is mainly used for identification of those acquisitions affected by clouds (Fig. 3a) and wave-focusing (Fig. 3b) occurrences or collected under very unstable sky conditions (Fig. 3c). Note that no measurement of the instrument attitude with respect to the vertical (Mueller et al. 2003) is available for this generation of Bio-Argo

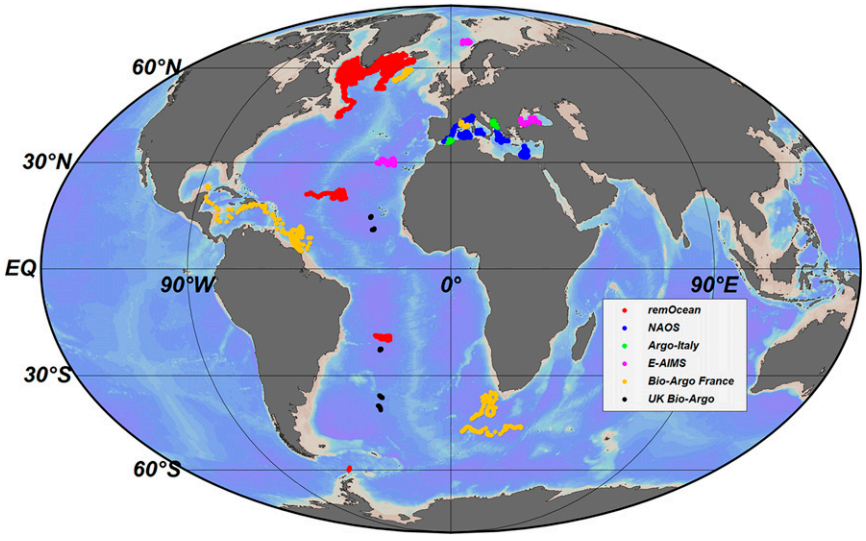

FIG. 2. Sampling stations obtained by 65 Bio-Argo floats between 8 Nov 2012 and 19 Nov 2014. Stations are grouped according to the research program. The map is drawn by the Ocean Data View software (R. Schlitzer, Ocean Data View, http://odv.awi.de).

floats, so any bad measurement occurring especially at shallowest depths because of the wave motion is managed here similarly to the wave-focusing effect. Flag 3 is further used for identifying those measurements corresponding to dark signal measured at depth (Fig. 3d). Flag 4 is dedicated only to potential failures of the radiometer in measuring and acquiring data correctly. The few measurements representing such a situation were preventively removed from the dataset we tested, so flag 4 is not included in the presented strategy of flag assignment.

Two important concepts have also to be kept in mind when developing Argo quality-control procedures. First, if flag 3 is assigned, the data should be later adjusted before any scientific utilization. Second, the flag assigned to a given data point can only be degraded (e.g., from 1 to 3) along with the various tests, but never requalified (e.g., from 3 to 1).

In addition, tests assessing the overall quality of the entire profile were also implemented. Each profile was assigned to one of the three selected categories (called "profile type"): "type 1" for good profiles, "type 2" for probably good profiles, and "type 3" for probably bad profiles. Analogously to flags assigned to each data point acquired along the profile, profiles classified as type 3 should be adjusted (corrected) before their use. According to these constraints, automatic quality-control tests were therefore developed.

4. Data analysis protocols

In the following sections, we present in detail protocols and criteria specifically designed and chosen for Bio-Argo radiometric measurements and applied to identify dark signal, atmospheric clouds, wave-focusing, and spike occurrences, and to evaluate the overall quality of the entire profile (i.e., profile type assignment).

a. Dark signal identification

The dark current of radiometric sensors is frequently measured in the deep part of a Bio-Argo profile. This offset needs to be identified and possibly corrected prior to further processing (Mueller et al. 2003). As this quality-control procedure is developed for bio-optical applications (e.g., analysis of the diffuse light attenuation coefficient $K_d(\lambda)$, ocean color radiometry validation), the upper layer of the water column is of larger interest than the deeper layer. The average impact of dark current values identified in each tested profile on the corresponding irradiance value measured at the ocean surface was negligible for all four radiometric channels (<1%). Hence, no dark offset adjustment was implemented in the quality-control procedure.

Dark values were identified by testing the normality of the distribution along the depth. The main assumption is that the upper part of the profile, corresponding to the effective light measurements, is not normally distributed as light decreases with depth, whereas the deep part of the profile corresponding to dark measurements is assumed to be normally distributed. This assumption was tested and verified for $E_d(\lambda)$ and PAR vertical profiles from various environmental conditions. Following the method by Wilk and Gnanadesikan (1968), the standardized distribution of the measured

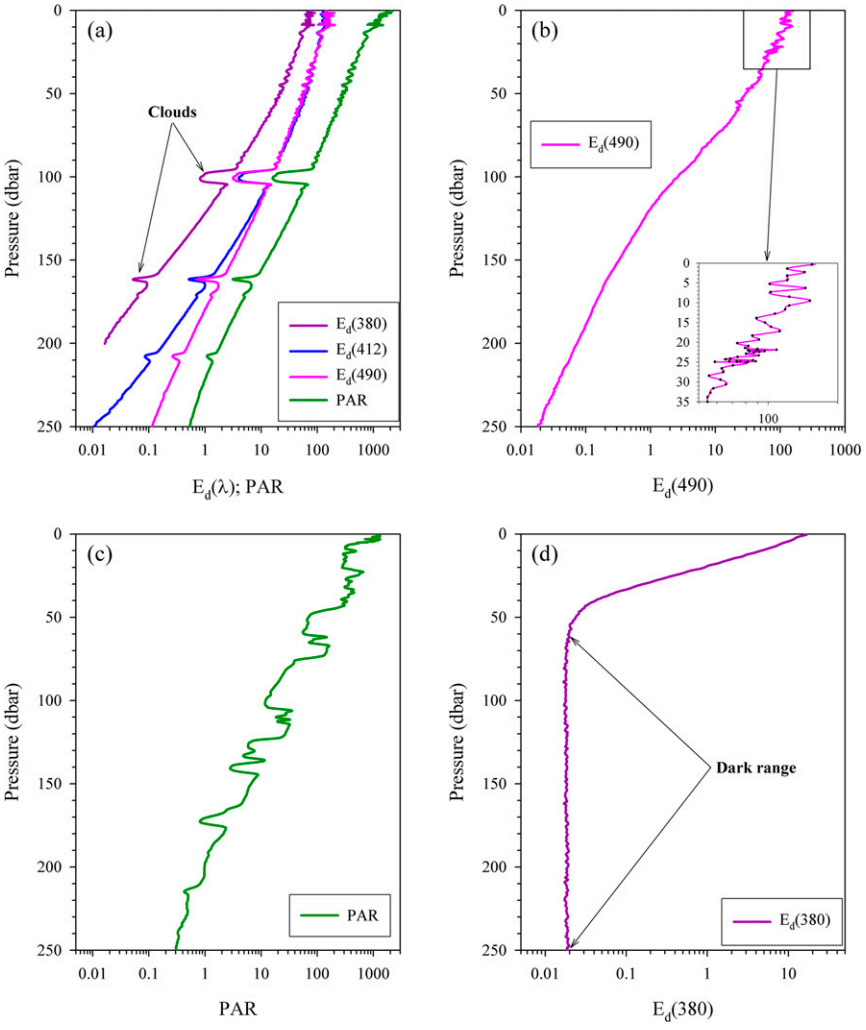

FIG. 3. Examples of (a) atmospheric cloud occurrence along profiles acquired by Bio-Argo floats (float WMO 6901439), (b) wave focusing in the surface layer (float WMO 6901655), (c) profile acquired in very unstable sky and sea conditions (float WMO 6901439), and (d) dark occurrence along the profile (float WMO 6901486). Values of $E_d(\lambda)$ at 380, 412, and 490 nm are expressed as $\mu W\,cm^{-2}\,nm^{-1}$. PAR values are expressed as μmol quanta $m^{-2}\,s^{-1}$. Depth is expressed in units of pressure.

dark values was compared to theoretical normally distributed values (see example in Fig. 4). The Lilliefors test (Thode 2002) for normality ($\alpha = 0.01$) was applied to irradiance or PAR values. Computation first included all measured values from 0 to 250 m of depth. Afterward, the Lilliefors test was applied on the same profile after removing the shallowest measured value. The value for which the remaining measurements were normally distributed was considered as the first value for the dark. The lower limit of the $E_d(\lambda)$ or PAR profile was, subsequently, set at this depth (Fig. 4a).

The choice of using such a profile-determined procedure, instead of cutting the profiles at a fixed value, was driven by various reasons. Because the sensor sensitivity can be affected by issues such as water temperature dependence (Mueller et al. 2003) or might change over radiometer lifetime (i.e., instrumental drift), the use of a minimum signal cutoff [e.g., noise equivalent irradiance (NEI) as provided by the manufacturer] failed in some occasions and no dark cutoff depth was selected (Fig. 4a). Actually, the average dark value measured in a profile, although generally very small [$<|0.08|\,\mu W\,cm^{-2}\,nm^{-1}$ for $E_d(\lambda)$], was different among radiometric sensors and channels. The advantage of the profile-by-profile approach is that it only considers how data are distributed and, more importantly, it can be

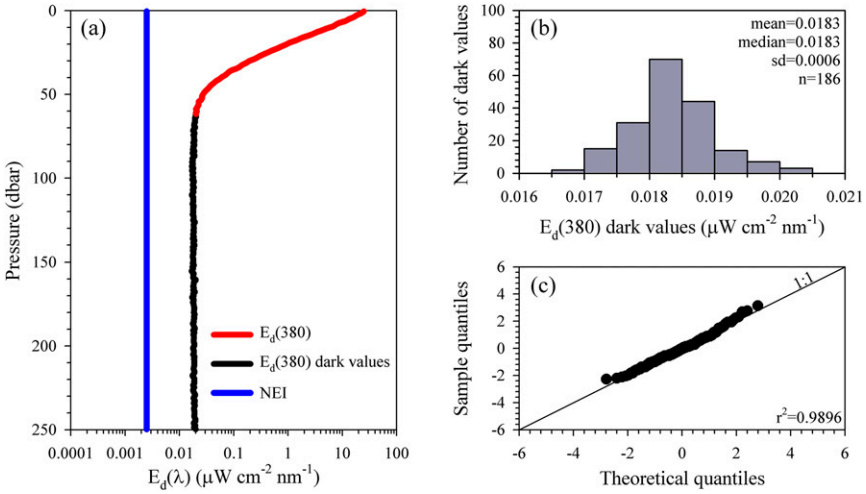

FIG. 4. (a) Example of dark values identified by the Lilliefors test of normality within a radiometric profile (float WMO 6901486). The NEI value specific for OCR-504 radiometers (SATLANTIC 2013) is shown for comparison. Depth is expressed in units of pressure. (b) Histogram of $E_d(380)$ dark values identified in (a); mean, median, standard deviation (sd), and number (n) of dark values are indicated. (c) Quantile–quantile scatterplot (Wilk and Gnanadesikan 1968) of standardized $E_d(380)$ dark values identified in (a) vs theoretical normally distributed values. Lack of deviation from the 1:1 ratio (solid line) confirms that dark measurements are normally distributed.

universally applied to all radiometric instruments at any wavelength. The procedure performance therefore depends on the shape of the profile. In addition, the procedure is totally insensitive to the possible drifts in NEI values that could occur over the expected radiometer lifetime.

The sensitivity of the method, however, was found to vary according to the number of dark values included in the distribution. For the example in Fig. 4a, the minimum cutoff dark value was found to be the same when testing both 0–250- and 0–120-m measurements. But, when the number of dark values was reduced more than 65%, the cutoff dark depth was observed to shallow. Hence, testing the entire available irradiance distribution (i.e., 0–250 m for this dataset) ensured the best performance in determining the dark cutoff limit for most environmental conditions we examined, although performance might be lower in the case of very clear waters with a low number of dark values in the 0–250-m layer (e.g., subtropical gyres).

b. Identification of clouds, wave focusing, and spikes

Because radiometric measurements by Bio-Argo floats are made automatically, regardless of meteorological sea and sky conditions, moving atmospheric clouds and a wave-focusing effect (Zaneveld et al. 2001) can perturb the in-water light field and affect the quality of measurements. It is important to recall that a good radiometric measurement useful to bio-optical applications can be acquired either in clear or fully overcast sky conditions, as long as they are constant. In addition, spikes might also occur and have to be detected.

Measurements affected by clouds, wave focusing, and spikes were identified as outliers among residual values produced with respect to a nonlinear fit on radiometric profiles after removal of dark measurements. A fourth-degree polynomial was fitted to the Napierian logarithm of $E_d(\lambda)$ or PAR profiles versus the depth indicated by the pressure measured in decibars (dbar). The records along the profile, with residual larger than ±1 or ±2 times the standard deviation from the mean of residuals, were then assigned to flags 2 or 3, respectively. This fit was effective in identifying most of the data affected by clouds and spikes. A second fit, using the same criteria, was performed on that part of the profile excluding data flagged as "3." This polynomial fit identified the variability induced by wave focusing at surface and minor clouds not identified by the first polynomial fit.

Evidence for choosing a fourth-degree polynomial function is provided in Fig. 5, where a comparison between linear, second-, and third-degree polynomial fits is shown. No degrees of the polynomial function higher than four were tested, as generally they are more sensitive to noisy values occurring at the surface (i.e., wave focusing) and to small values close to dark signal at depth. The linear fit typically provided the worst interpolations of downward irradiance and PAR profiles (Figs. 5a,b). Its performance appeared to be strongly

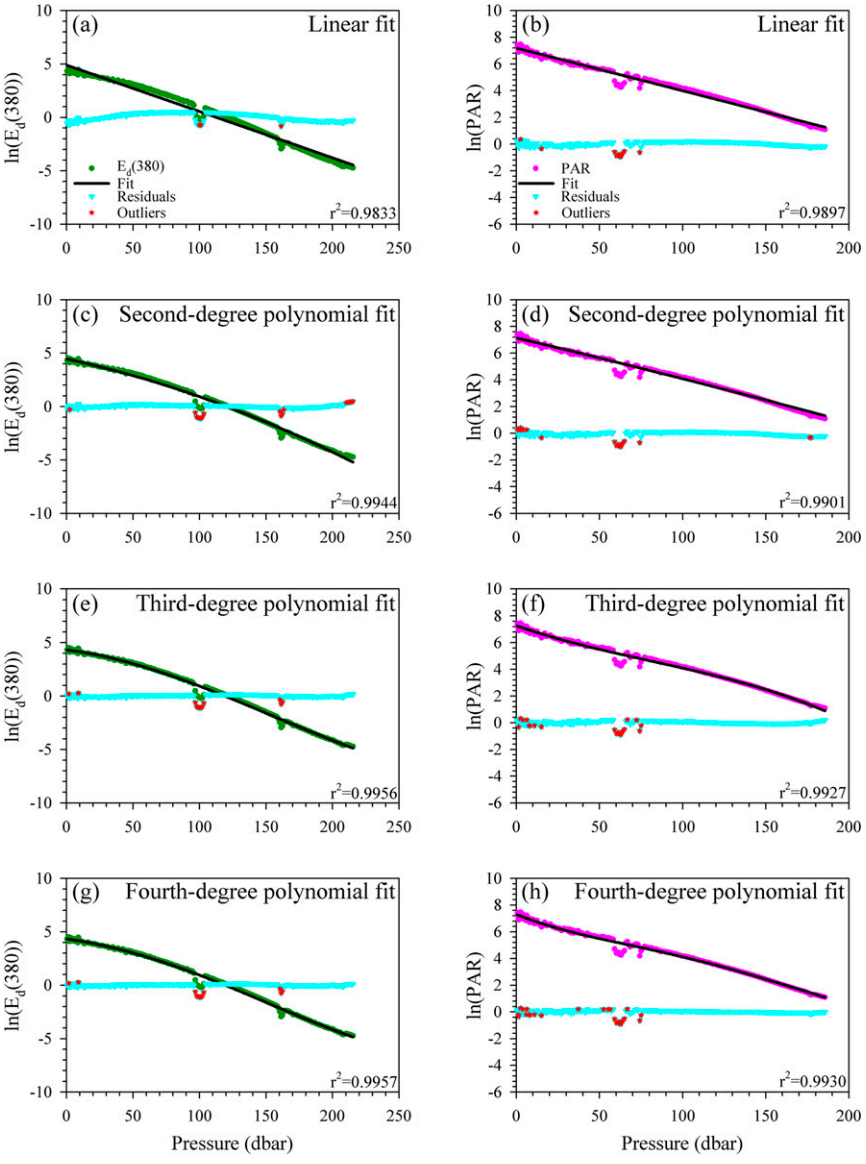

FIG. 5. Examples of radiometric profiles fitted by (a),(b) linear function; (c),(d) second-degree polynomial function; (e),(f) third-degree polynomial function; and (g),(h) fourth-degree polynomial function. Examples are displayed for downward irradiance at 380 nm (float WMO 6901439) and PAR (float WMO 6901440) after removal of dark values. Residuals and outliers (points out ±2 times the standard deviation from the mean of residuals) are also shown on the same axes. Depth is expressed in units of pressure.

dependent on the perturbation given by clouds overpassing during the measurement (Fig. 5a). The three polynomial functions were found to fit irradiance and PAR profiles better than the linear one (Figs. 5c–h). Determination coefficients (r^2) also improved with increasing degree number. More importantly, the polynomial function was found to be less sensitive to cloud-induced light perturbations, offering a possible way for their identification. The second- and third-degree polynomial fits were not able to accurately reproduce the whole radiometric profiles at their extremities and showed different performance depending on the radiometric channel (Figs. 5c–f). In contrast, the fourth-degree polynomial fit performed accurately over the whole profile (extremities included; Figs. 5g,h) in a similar way for all four radiometric channels. Furthermore, the fourth-degree polynomial fit was able to reproduce, better than the other tested functions, those radiometric profiles showing two chlorophyll maxima at depth (data not shown).

TABLE 1. Thresholds of r^2 used for profile type identification.

Channel	Type 3	Type 2	Type 1
$E_d(380)$	$r^2 \le 0.997$	$0.997 < r^2 \le 0.999$	$r^2 > 0.999$
$E_d(412)$	$r^2 \le 0.997$	$0.997 < r^2 \le 0.998$	$r^2 > 0.998$
$E_d(490)$	$r^2 \le 0.996$	$0.996 < r^2 \le 0.998$	$r^2 > 0.998$
PAR	$r^2 \le 0.996$	$0.996 < r^2 \le 0.998$	$r^2 > 0.998$

c. *Profile type assignment*

Profile type identification was achieved by using a simple criterion based on determination coefficients obtained from the polynomial fits. Thanks to a first test applied to all the radiometric channels, r^2 lower than 0.995 was used as the criterion for identifying type 3 profiles. Then, when the second fourth-degree polynomial fit was computed on partially cleaned profiles, increasing thresholds of r^2 values (Table 1) were used to identify additional type 3 profiles that passed the previous test, but also type 2 and type 1 profiles. The thresholds used for the profile type identification were adapted for each radiometric channel (Table 1) with the help of a visual test on more than 4000 profiles in order to ensure the best identification of each profile type.

5. Procedure overview

An overview of the procedure showing the various steps and the sequence of the various tests (reported in section 4) for flag and profile type assignments is given in Fig. 6. This procedure, specifically designed for Bio-Argo radiometric measurements, is exactly the same for each channel [PAR and $E_d(\lambda)$] and for each profile.

In step 0, a test based on the solar elevation, calculated at the end of the cast, identifies those profiles acquired at night (e.g., during multiprofiling float missions), all records are flagged as "3" ("type 3" profile), and the processing stops (Fig. 6).

Step 1 identifies the possible dark values measured during the cast. No dark offset adjustments are implemented. Values identified as dark are flagged as "3" and are no longer tested (Fig. 6). A second test checks the number of records remaining along the profile after identification of the dark signal. If the number of measured points is lower than 5, thus equal to or lower than the degree of polynomial fit used to identify any perturbation of the light field (e.g., clouds), then all the records along the profile are flagged as "3," the profile is classified as "type 3," and the processing stops.

In step 2, a polynomial fit is performed using all values (except the dark values) within the profile. Then, the first test based on r^2 (see section 4c) identifies if the

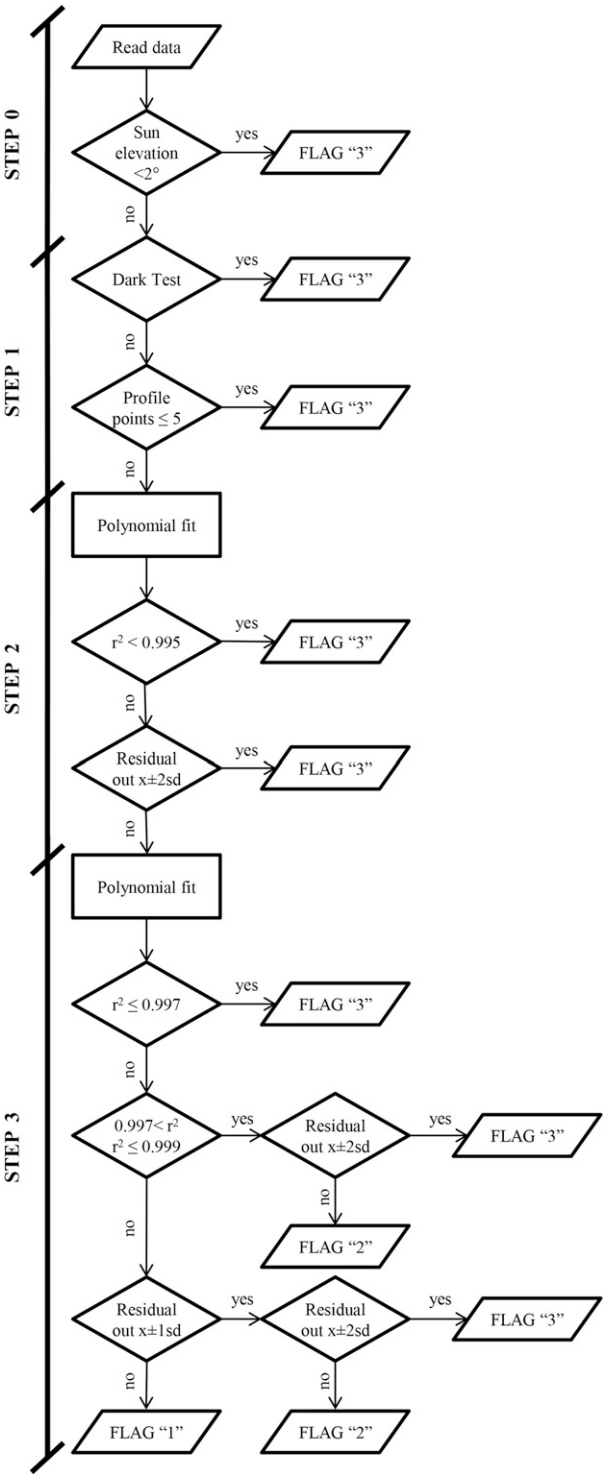

FIG. 6. Flowchart of the QC procedure for radiometric data acquired by Bio-Argo floats [e.g., $E_d(380)$]; "x" is the mean of residuals.

current profile has been acquired under very unstable sky and sea conditions (i.e., type 3). In this case, all records acquired during the cast are flagged as "3" and the processing stops (Fig. 6). If the profile is not classified as a probably bad profile, then each spike or record affected by clouds is assigned to the flag category 3 and no longer tested. The remaining records are flagged as "1."

Along step 3, the points of the profile flagged as "1" are used to fit again the $E_d(\lambda)$ or PAR profile by a polynomial function. A test based on the first r^2 threshold listed in Table 1 (see section 4c) is performed to test again if the profile was collected under very unstable sky and sea conditions (i.e., type 3). If the profile is classified as type 3, then all records acquired during the cast are flagged as "3" and the processing stops (Fig. 6). If the profile passes this test, then a further check based on the second r^2 threshold listed in Table 1 evaluates if the profile must be considered as probably good (i.e., type 2). In this case all tested records are first flagged as "2" and then as "3" if they are affected by wave focusing or minor clouds. If, along step 3, the profile is overall considered as good (i.e., type 1), then all tested points are first flagged as "1" and then flags 2 and 3 are assigned for points corresponding to waves and any cloud residual perturbations. At the end of step 3, the routine stops processing and the QC profile is generated.

6. Results of the quality-control procedure

a. *Cleaning for dark signal, clouds, and wave-focusing effect*

The quality-control procedure was applied on 26 280 profiles (6570 for each radiometric channel) collected in a large range of oceanic conditions (Fig. 2). The performance of the QC procedure in identifying clouds, wave focusing, and dark occurrences was evaluated. To illustrate the effectiveness of the procedure, example profiles are presented for different environmental conditions and radiometric channels in Fig. 7. All selected radiometric measurements were affected by clouds and wave focusing as main perturbations (Fig. 7). In addition, dark values were often identified in the lower part of the profile. The normality test for removing the dark signal and the analysis of residuals on a fourth-degree polynomial fit efficiently detected the various perturbations. Corrected profiles were, therefore, provided (Fig. 7).

The developed QC procedure was independent of the radiometric channel analyzed and insensitive to the measured light intensities (Fig. 7), which makes it applicable at global scale. However, the QC procedure showed sporadic lower performances. Two main causes were identified. 1) Dark values were erroneously considered as good values by the normality test. In this case, the presence of the measurement in the dark range could actually affect the performances of the polynomial fit, such that the identification of clouds and other perturbations could be seriously invalidated. 2) The occurrence of slow-moving clouds induced a wavy behavior of the radiometric profile that was hard to detect.

b. *Overall quality of the profiles*

QC procedure performances were also evaluated by assessing the overall quality of vertical profiles (as opposed to a single measurement at a given depth). Examples of various profiles classified from type 1 to type 3 are shown in Fig. 8 for two different environments (North Atlantic Subpolar Gyre and South Atlantic Subtropical Gyre). It is important to keep in mind that the profile type is assigned after removing the major perturbations, such as clouds. Results of the QC application revealed that 60% of the 26 280 profiles were considered as belonging to type 1 (Fig. 8a; Table 2), that is, profiles that did not require any further modification and could be immediately used. Type 2 profiles—that is, those with potentially usable measurements—represented on average 15% of all the profiles (Fig. 8b; Table 2). Type 3 profiles—that is, those that should be adjusted before being used—represented 25% of the whole database (Fig. 8c; Table 2). However, when analyzing specifically each radiometric channel (Table 2), the performances of the procedure differed and the various profile types were assigned in different proportions. This is because the signal-to-noise ratio is specific for a given radiometric channel. Moreover, because the irradiance penetration depths vary as a function of wavelength, each radiometric channel might meet with a different number of perturbations (e.g., clouds) during the cast (see example in Fig. 3a), and this can affect the determination coefficient of the polynomial fit used to assign a given profile type. For example, the QC procedure for $E_d(412)$ data returned a higher number of type 1 profiles (67%) and a lower fraction of type 2 profiles (9%) than for the other channels (Table 2). For $E_d(380)$, the number of type 2 profiles was higher (22%) than for other channels. The proportions of the various profile types were similar between $E_d(490)$ and PAR (Table 2).

7. Surface incident irradiance from QC profiles

The quality-control procedure presented in the previous sections analyzed and verified only the shape of a radiometric profile and its perturbations (e.g., clouds). No quality control on the absolute value of the measured quantity was performed. To verify the accuracy of

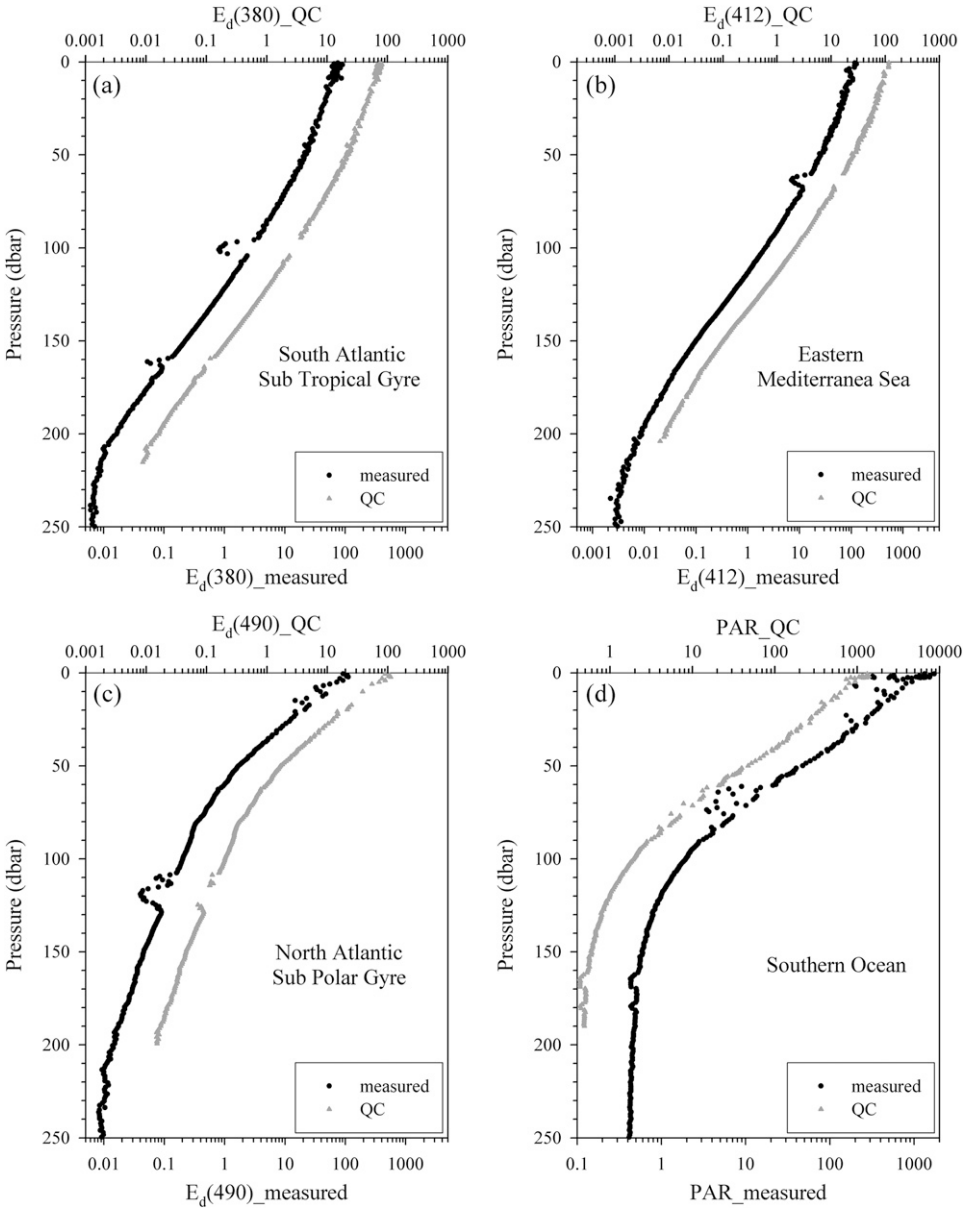

FIG. 7. Examples of vertical profiles before and after QC processing (only points flagged as "1" and "2" are shown): (a) $E_d(380)$ from float WMO 6901439 (South Atlantic Subtropical Gyre); (b) $E_d(412)$ from float WMO 6901528 (eastern Mediterranean Sea); (c) $E_d(490)$ from float WMO 6901485 (North Atlantic Subpolar Gyre); and (d) PAR from float WMO 6901492 (Southern Ocean). Values of $E_d(\lambda)$ are expressed as $\mu W\,cm^{-2}\,nm^{-1}$. PAR values are expressed as $\mu mol\,quanta\,m^{-2}\,s^{-1}$. Measured and QC profiles are displayed on different x axes only for improved visualization. Depth is expressed in units of pressure.

the measurements, incident irradiance values above the surface $E_d(0^+)$ from quality-controlled Bio-Argo radiometry profiles were compared to theoretical clear-sky $E_d(0^+)$ values computed according to Gregg and Carder (1990). For all type 1 profiles, downward irradiance values just below the surface $[E_d(0^-)]$ were first calculated through extrapolation within the first penetration depth (as defined by Gordon and McCluney 1975) using a second-degree polynomial function. The $E_d(0^-)$ estimates by such a function within the first penetration depth were found to fit closer to true values than usual log-linear extrapolations (D. Antoine 2015, personal communication). The $E_d(0^-)$ values were then converted into $E_d(0^+)$ values by dividing for the transmission across the sea–air interface factor following Austin (1974).

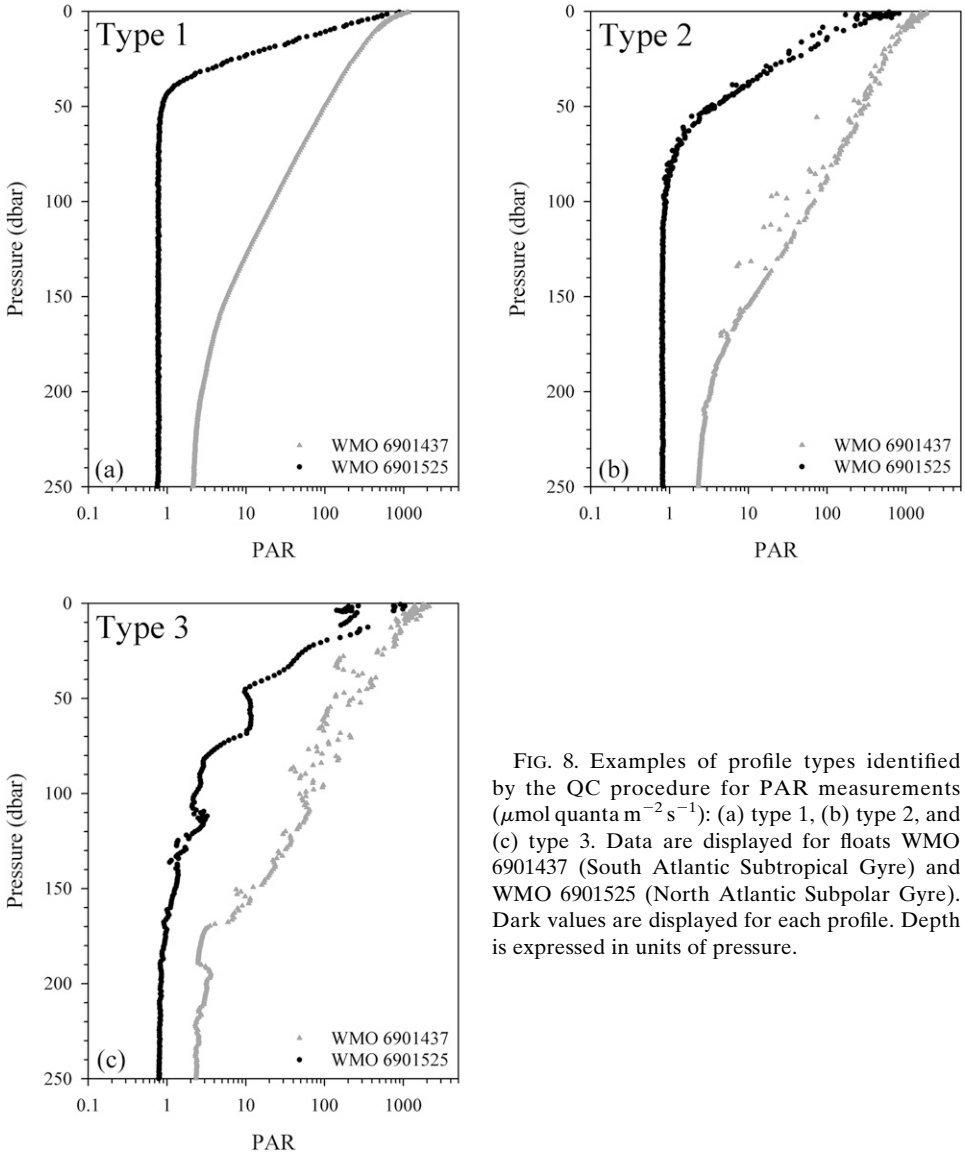

FIG. 8. Examples of profile types identified by the QC procedure for PAR measurements (μmol quanta m^{-2} s^{-1}): (a) type 1, (b) type 2, and (c) type 3. Data are displayed for floats WMO 6901437 (South Atlantic Subtropical Gyre) and WMO 6901525 (North Atlantic Subpolar Gyre). Dark values are displayed for each profile. Depth is expressed in units of pressure.

Good agreement was generally observed between modeled and in situ incident surface solar irradiances at 380, 412, and 490 nm (Fig. 9). Fluctuations observed in $E_d(0^+)$ values extrapolated at the surface from Bio-Argo measurements mostly reflected the occurrence of cloudy days and thus justified divergences from modeled values. The systematic error (Bias) and the relative root-mean-square error (RMSE%) were calculated between modeled and in situ irradiance maxima over a window of seven consecutive measurements in order to remove the influence of cloudy days (Fig. 9; Table 3). For the majority of floats, the $E_d(0^+)$ in situ values kept in agreement with the modeled ones for all the radiometric channels even after more than one year from the date of deployment (examples from two floats profiling every 10 days are shown in Figs. 9a–f). Indeed, the bias between modeled and in situ irradiance maxima was similar over the time series for the three wavelengths (Figs. 9a–f). In contrast, in some cases the bias varied along the float lifetime because of instrumental drift and biofouling

TABLE 2. Number of profiles (expressed in percentage) assigned to each profile type.

Channel	Type 1	Type 2	Type 3
$E_d(380)$	58%	22%	20%
$E_d(412)$	67%	9%	24%
$E_d(490)$	56%	15%	29%
PAR	57%	16%	27%
All	60%	15%	25%

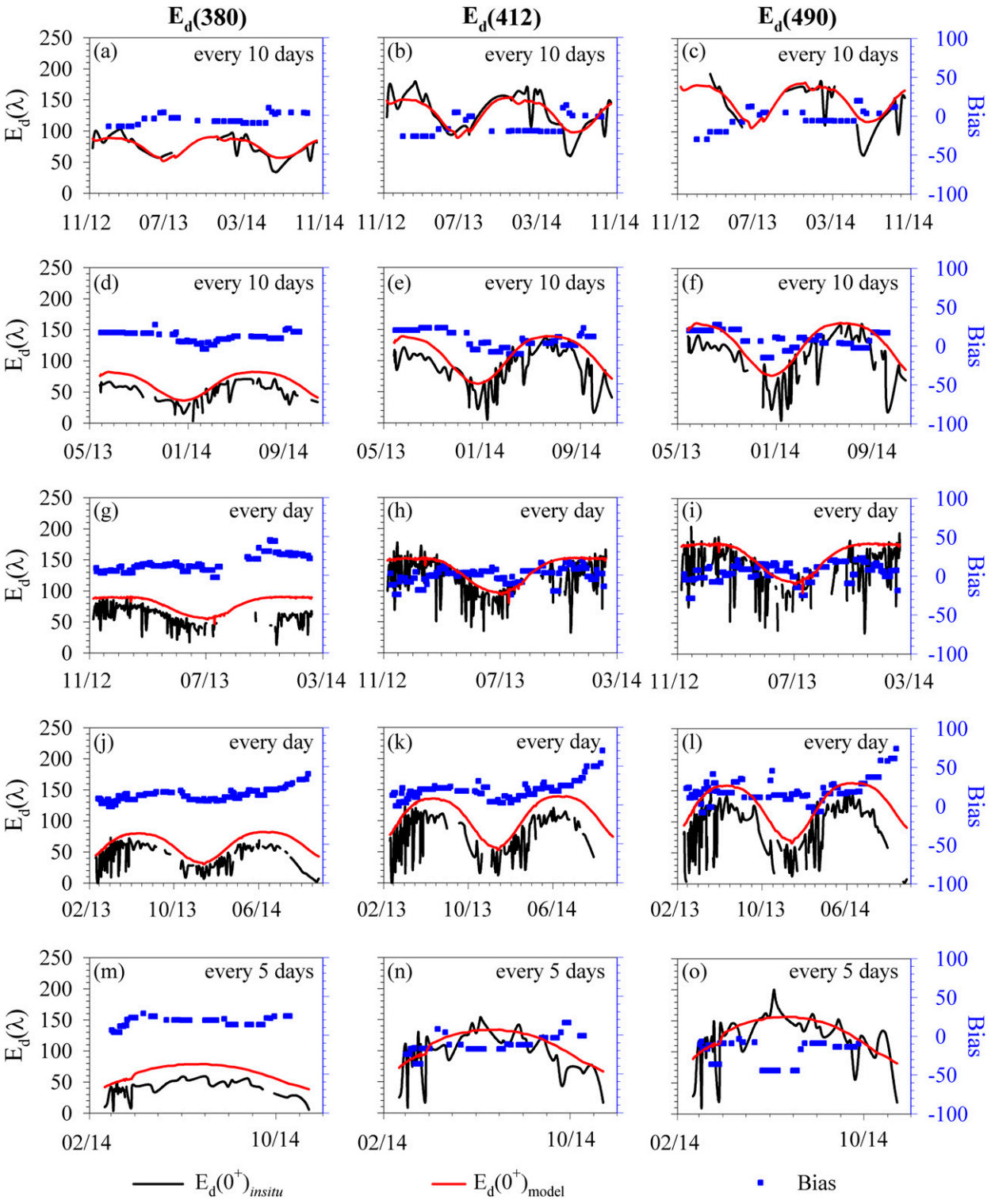

FIG. 9. Comparison between theoretical clear-sky surface incident irradiance values above the surface $[E_d(0^+)_{model}]$ computed according to Gregg and Carder (1990) and above-surface incident irradiance values extrapolated from type 1 quality-controlled Bio-Argo radiometric profiles $[E_d(0^+)_{insitu}]$. Comparisons are displayed for $E_d(\lambda)$ (μW cm^{-2} nm^{-1}) at (left) 380, (middle) 412, and (right) 490 nm, and for five Bio-Argo floats: (a)–(c) WMO 6901437 (South Atlantic Subtropical Gyre); (d)–(f) WMO 6901510 (eastern Mediterranean Sea); (g)–(i) WMO 6901439 (South Atlantic Subtropical Gyre); (j)–(l) WMO 6901511 (western Mediterranean Sea); (m)–(o) WMO 6901865 (eastern Mediterranean Sea). Each panel shows the main frequency of the profile acquisition and Bias (μW cm^{-2} nm^{-1}) between the modeled and in situ irradiance maxima over a window of seven consecutive measurements.

TABLE 3. Systematic error (bias; $\mu W\,cm^{-2}\,nm^{-1}$) and RMSE% for $E_d(0^+)$ time series displayed in Fig. 9. Bias and RMSE% were calculated between modeled and in situ irradiance maxima over a window of seven consecutive measurements.

		Bias[a]			RMSE%[a]		
Float WMO	n	$E_d(380)$	$E_d(412)$	$E_d(490)$	$E_d(380)$	$E_d(412)$	$E_d(490)$
6901437	33	−5.09	−13.46	−2.76	10%	13%	8%
6901510	73	9.87	4.21	7.06	18%	10%	9%
6901439	241[b]	15.14	−0.93	3.76	23%	7%	8%
6901511	172	10.93	16.00	17.34	20%	17%	17%
6901865	47[c]	15.76	−15.33	−20.58	27%	19%	19%

[a] Systematic error and relative root-mean-square error are calculated as Bias $= \sum_{i=1}^{n}(\hat{x}_i - x_i)/n$ and RMSE% $= 100/\bar{x} \times [\sum_{i=1}^{n}(\hat{x}_i - x_i)^2/n]^{1/2}$, respectively, where $\hat{x}_i$ is the modeled value, x_i is the measured value, $\bar{x}$ is the average of modeled values, and n is the number of data.
[b] $n = 219$ for $E_d(380)$.
[c] $n = 44$ for $E_d(490)$.

(i.e., growth of organisms on the collectors). For example, in the case of a float deployed in the South Atlantic Subtropical Gyre, the channel measuring $E_d(380)$ appeared to be affected probably by biofouling, likely together with instrumental drift, after 9 months from the deployment because the difference between the modeled and in situ values was found to increase (Fig. 9g; Table 3). Note that this float, contrary to others, was profiling daily and thus it spent on average less time at the parking depth (1000 m), where conditions of high pressure, absence of light, and cold temperatures are unfavorable for growth. Biofouling was instead observed to occur simultaneously for all the radiometric channels after 1 year at sea for a float in the western Mediterranean Sea, as suggested by the simultaneous increase of the bias for the three wavelengths (Figs. 9j–l). Also, this float spent less time at the parking depth, likely supporting organism growth on sensors. In the case of a float operating in the eastern Mediterranean Sea (Figs. 9m–o), probably calibration errors affected the accuracy of downward irradiance measurements at 380 nm (Fig. 9m), while $E_d(0^+)$ values measured by the other radiometric channels were in agreement with modeled $E_d(0^+)$ values (Figs. 9n,o). The bias did not vary over the time for the three wavelengths, but the RMSE% value estimated for the channel 380 nm was higher than those observed for the other channels (Figs. 9n,o; Table 3). In conclusion, these comparisons were useful for evaluating the performances of the radiometers and thus the accuracy of the measurements over the lifetime of the float.

8. Summary and future directions

Bio-Argo profiling floats represent a highly innovative way to acquire in situ radiometric profiles. This new observation technology promises advances in the field of biological (e.g., for modeling primary production) and optical (e.g., for bio-optical modeling and ocean color product validation) oceanography. Since the first radiometric measurement by a PROVOR CTS-4 float in November 2012, an array of 65 of such floats yielded thousands of in situ profiles of downward irradiance at three wavelengths and PAR (more than 26 000 acquisitions in two years) in several oceanic areas representative of the diversity of trophic and bio-optical conditions prevailing in the so-called case 1 waters (Morel and Prieur 1977). The rationale for such Bio-Argo float deployment was generally to focus on traditionally undersampled areas (e.g., North Atlantic) or remote zones (e.g., subtropical gyres) or regions characterized by contrasting trophic regimes (e.g., Mediterranean Sea; D'Ortenzio and Ribera d'Alcalà 2009). For the community of biological and optical oceanographers, it has already produced a unique dataset from the surface to the ocean interior with unprecedented spatiotemporal resolution.

Observations made by Bio-Argo floats, however, are performed out of an operator's control and regardless of meteorological conditions. Whereas these sampling circumstances are of less importance for measurements of variables, such as chlorophyll fluorescence and nitrate concentrations, they are critical for radiometric measurements. While, for instance, the vertical distribution of nitrates is not affected by atmospheric clouds during the measurement, the response of the in-water light field is instead instantaneous. Profiles that would be disregarded or repeated in the frame of a traditional sampling made by an operator on a ship are instead retained by the profiling float and transmitted to the operator. Quality control is, therefore, mandatory.

Standard protocols for quality-controlling radiometric measurements (Mueller et al. 2003) are only partially applicable to this new way of measuring the light field in the ocean. The main causes are the lack of simultaneous above-water surface irradiance measurements and the lack of routinely dark instrument readings. Recommended

protocols were therefore adapted to Bio-Argo radiometric measurements. The specific procedure essentially consisted of a series of automatic statistical and mathematical tests aimed at identifying dark signal measured at depth, clouds, or noise due to light refracted by waves at the surface. Profiles acquired under unstable sky conditions were also identified. The procedure, which flagged each measured irradiance value in a way compliant with the international Argo data management system, revealed to be adapted to each of the four radiometric channels [i.e., $E_d(380)$, $E_d(412)$, $E_d(490)$, PAR], thus suggesting its potential applicability to any wavelength and to all Bio-Argo radiometric instruments sharing the same measurements principles of the sensors used in this implementation. Good performance was achieved for the entire dataset of 26 280 radiometric profiles collected across the oceans. More importantly, the quality-control system correctly identified the main perturbations regardless of the light intensity or vertical distribution of the radiometric field, thus suggesting its applicability at the global scale.

According to the Argo data management system (Wong et al. 2013), each variable acquired by Bio-Argo floats is expected to be quality-controlled and distributed to the community in real time and within 24 h from sampling. Subsequently, a further quality control can be performed and directed at a detailed review of the data (i.e., delayed-mode quality control; Schmid et al. 2007). The procedure, presented here, was set up to automatically verify the quality of the measurements and to provide the distribution of data in real time. Severe criteria were implemented in order to achieve the best performance. Sixty percent of the measured profiles were eventually kept. It is important to note that for biogeochemical applications (e.g., feeding photosynthesis models), this strict quality control is not required and profiles can be used regardless of assigned flags. On the contrary, in the context of bio-optical applications focused at studying the upper layer of the oceans, the availability of a high number of strictly quality-controlled radiometric profiles in a very short time could represent a fruitful resource for several applications. In effect, efforts are underway for exploiting real-time radiometry-derived products [i.e., diffuse light attenuation coefficients, $K_d(\lambda)$] for defining the bio-optical status of the oceans, that is, delineating oceanic regions with optical properties departing from global bio-optical relationships (e.g., Morel and Maritorena 2001; Morel et al. 2007). Efforts are pursued also for using real-time quality-controlled products as a data source for constantly validating ocean color products [e.g., $K_d(490)$] in very different open ocean systems. In this context, following the recommendation of the International Ocean Colour Coordinating Group (Claustre 2011), floats specifically designed and equipped with radiometers matching current satellite bands are also under construction and will complement the existing array of Bio-Argo floats soon (http://www.obs-vlfr.fr/OAO/).

Others factors such as biofouling and instrumental drift, which are not taken into account in the presented quality-control procedure, could affect performance of the radiometer and therefore the quality of irradiance profiles. These issues, however, can be detected and assessed during the life of a float or at the end of the mission. The ''delayed mode'' control is currently planned for correction of these problems. Efforts are already directed toward the assessment of these perturbations as well as toward the adaptation of methods typically used for correcting data collected by moored and drifting buoys (Kuwahara et al. 2003; Antoine et al. 2008). A list of future delayed-mode quality-control actions on radiometric data measured by Bio-Argo floats will be directed also to dark instrument corrections, assessment of the sensor sensitivity to changes in temperature, and recovery of those profiles misclassified in the real-time quality-control phase. A fully quality-controlled dataset of radiometric profiles acquired by Bio-Argo floats will, therefore, be compiled on behalf of the community and for the benefit of biological and optical oceanography.

Acknowledgments. We are grateful to the valuable work of Grigor Obolensky (Laboratoire d'Océanographie de Villefranche and Ifremer Brest, France), who deployed most of Bio-Argo floats in many different oceanic areas. This study is a contribution to several projects: remOcean (funded by the European Research Council, Grant Agreement 246777), NAOS (funded by the Agence Nationale de la Recherche in the frame of the French ''Equipement d'avenir'' program, Grant Agreement ANR J11R107-F), U.K. Bio-Argo [funded by the Natural Environment Research Council (NERC)], Argo-Italy [funded by the Italian Ministry of Education, University and Research (MIUR)], E-AIMS (funded by European Commission's FP7 project), AtlantOS (funded by European Commission's H2020 program, Grant Agreement 2014-633211), and the French Bio-Argo program (Bio-Argo France; funded by CNES-TOSCA, LEFE Cyber, and GMMC). We thank the PIs of several Bio-Argo floats missions and projects: Hubert Loisel (Laboratoire d'Océanologie et de Géosciences, France; E-AIMS); Kjell-Arne Mork (Institute of Marine Research, Norway; E-AIMS); Pierre-Marie Poulain (National Institute of Oceanography and Experimental Geophysics, Italy; Argo-Italy); Violeta Slabakova (Bulgarian Academy of Sciences, Bulgaria; E-AIMS);

Emil Stanev (University of Oldenburg, Germany; E-AIMS); Sabrina Speich (Laboratoire de Météorologie Dynamique, France; Bio-Argo France); Virginie Thierry (Ifremer, France; Bio-Argo France); Pascal Conan (Observatoire Océanologique de Banyuls sur mer, France; Bio-Argo France); and Laurent Coppola (Laboratoire d'Océanographie de Villefranche, France; Bio-Argo France). All data presented in this study are publicly available online (at http://doi.org/10.17882/43499). The authors declare no conflicts of interest.

REFERENCES

Antoine, D., F. D'Ortenzio, S. B. Hooker, G. Bécu, B. Gentili, D. Tailliez, and A. J. Scott, 2008: Assessment of uncertainty in the ocean reflectance determined by three satellite ocean color sensors (MERIS, SeaWiFS, and MODIS-A) at an offshore site in the Mediterranean Sea (BOUSSOLE project). *J. Geophys. Res.*, **113**, C07013, doi:10.1029/2007JC004472.

Austin, R. W., 1974: The remote sensing of spectral radiance from below the ocean surface. *Optical Aspects of Oceanography*, N. G. Jerlov and E. Steemann-Nielsen, Eds., Elsevier, 317–344.

Bishop, J. K. B., and T. J. Wood, 2009: Year-round observations of carbon biomass and flux variability in the Southern Ocean. *Global Biogeochem. Cycles*, **23**, GB2019, doi:10.1029/2008GB003206.

Boss, E., D. Swift, L. Taylor, P. Brickley, R. Zaneveld, S. Riser, M. J. Perry, and P. G. Strutton, 2008: Observations of pigment and particle distributions in the western North Atlantic from an autonomous float and ocean color satellite. *Limnol. Oceanogr.*, **53**, 2112–2122, doi:10.4319/lo.2008.53.5_part_2.2112.

Claustre, H., Ed., 2011: Bio-optical sensors on Argo floats. IOCCG Report Series 11, 89 pp.

——, and Coauthors, 2010a: Bio-optical profiling floats as new observational tools for biogeochemical and ecosystem studies: Potential synergies with ocean color remote sensing. *Proceedings of OceanObs'09: Sustained Ocean Observations and Information for Society*, J. Hall, D. E. Harrison, and D. Stammer, Eds., Vol. 2, ESA Publ. WPP-306, doi:10.5270/OceanObs09.cwp.17.

——, and Coauthors, 2010b: Guidelines towards an integrated ocean observation system for ecosystems and biogeochemical cycles. *Proceedings of OceanObs'09: Sustained Ocean Observations and Information for Society*, J. Hall, D. E. Harrison, and D. Stammer, Eds., Vol. 1, ESA Publ. WPP-306, doi:10.5270/OceanObs09.pp.14.

D'Ortenzio, F., and M. Ribera d'Alcalà, 2009: On the trophic regimes of the Mediterranean Sea: A satellite analysis. *Biogeosciences*, **6**, 139–148, doi:10.5194/bg-6-139-2009.

Freeland, H. J., and Coauthors, 2010: Argo—A decade of progress. *Proceedings of OceanObs'09: Sustained Ocean Observations and Information for Society*, J. Hall, D. E. Harrison, and D. Stammer, Eds., Vol. 2, ESA Publ. WPP-306, doi:10.5270/OceanObs09.cwp.32.

Gordon, H. R., and W. R. McCluney, 1975: Estimation of the depth of sunlight penetration in the sea for remote sensing. *Appl. Opt.*, **14**, 413–416, doi:10.1364/AO.14.000413.

Gregg, W. W., and K. L. Carder, 1990: A simple spectral solar irradiance model for cloudless maritime atmospheres. *Limnol. Oceanogr.*, **35**, 1657–1675, doi:10.4319/lo.1990.35.8.1657.

Johnson, K. S., and Coauthors, 2009: Observing biogeochemical cycles at global scales with profiling floats and gliders: Prospects for a global array. *Oceanography*, **22** (3), 216–225, doi:10.5670/oceanog.2009.81.

Körtzinger, A., J. Schimanski, U. Send, and D. Wallace, 2004: The ocean takes a deep breath. *Science*, **306**, 1337, doi:10.1126/science.1102557.

Kuwahara, V. S., and Coauthors, 2003: Radiometric and bio-optical measurements from moored and drifting buoys: Measurement and data analysis protocols. Special topics in ocean optics protocols and appendices, J. L. Mueller, G. S. Fargion, and C. R. McClain, Eds., Vol. VI, Rev. 4, Ocean optics protocols for satellite ocean color sensor validation, NASA Tech. Memo. NASA/TM-2003-211621/Rev-Vol VI, 35–78.

Morel, A., and L. Prieur, 1977: Analysis of variations in ocean color. *Limnol. Oceanogr.*, **22**, 709–722, doi:10.4319/lo.1977.22.4.0709.

——, and S. Maritorena, 2001: Bio-optical properties of oceanic waters: A reappraisal. *J. Geophys. Res.*, **106**, 7163–7180, doi:10.1029/2000JC000319.

——, Y. Huot, B. Gentili, J. Werdell, S. B. Hooker, and B. A. Franz, 2007: Examining the consistency of products derived from various ocean color sensors in open ocean (Case 1) waters in the perspective of a multi-sensor approach. *Remote Sens. Environ.*, **111**, 69–88, doi:10.1016/j.rse.2007.03.012.

Mueller, J. L., and Coauthors, 2003: Radiometric measurements and data analysis protocols. Vol. 3, Rev. 4, J. L. Mueller, G. S. Fargion, and C. R. McClain, Eds., Ocean optics protocols for satellite ocean color sensor validation, NASA Tech. Memo. NASA/TM-2003-21621/Rev-Vol III, 78 pp.

Organelli, E., and Coauthors, 2016: Near-real-time quality-controlled radiometric profiles acquired by Bio-Argo floats. SEANOE, accessed 20 April 2016, doi:10.17882/43499.

SATLANTIC, 2013: Operation manual for the OCR-504. SATLANTIC Operation Manual SAT-DN-00034, Rev. G, 66 pp.

Schmid, C., R. L. Molinari, R. Sabina, and Y. Daneshzadeh, 2007: The real-time data management system for Argo profiling float observations. *J. Atmos. Oceanic Technol.*, **24**, 1608–1628, doi:10.1175/JTECH2070.1.

Thode, H. C., Jr., 2002: *Testing for Normality*. Statistics, Textbooks and Monographs, Vol. 164, Marcel Dekker, 479 pp.

Wilk, M. B., and R. Gnanadesikan, 1968: Probability plotting methods for the analysis of data. *Biometrika*, **55**, 1–17.

Wong, A., R. Keeley, and T. Carval, and the Argo Data Management Team, 2013: Argo quality control manual. Version 2.8, 50 pp. [Available online at http://www.argodatamgt.org/content/download/15699/102401/file/argo-quality-control-manual-version2.8.pdf.]

Xing, X., A. Morel, H. Claustre, D. Antoine, F. D'Ortenzio, A. Poteau, and A. Mignot, 2011: Combined processing and mutual interpretation of radiometry and fluorometry from autonomous profiling Bio-Argo floats. The retrieval of Chlorophyll *a*. *J. Geophys. Res.*, **116**, C06020, doi:10.1029/2010JC006899.

——, ——, ——, F. D'Ortenzio, and A. Poteau, 2012: Combined processing and mutual interpretation of radiometry and fluorometry from autonomous profiling Bio-Argo floats: 2. Colored dissolved organic matter absorption retrieval. *J. Geophys. Res.*, **117**, C04022, doi:10.1029/2011JC007632.

Zaneveld, R., E. Boss, and A. Barnard, 2001: Influence of surface waves on measured and modeled irradiance profiles. *Appl. Opt.*, **40**, 1442–1449, doi:10.1364/AO.40.001442.